Eur. Phys. J. E (2017) **40**: 82
DOI 10.1140/epje/i2017-11565-9

THE EUROPEAN PHYSICAL JOURNAL E

Regular Article

The equation of state of polymers. Part III: Relation with the compensation law

Jacques Rault[a]

Laboratoire de Physique des Solides, CNRS, Université de Paris-Sud, Orsay, 91405, France

Received 14 April 2017

Abstract. The properties of amorphous polymers and of organic compounds under pressure are interpreted in the framework of the modified Van der Walls Equation of State (mVW-EOS) the Vogel-Fulcher-Tamann (VFT) law and of the compensation law. We have shown recently that polymers and organic compounds in amorphous liquid and crystalline states verify the mVW-EOS which depends on three parameters, P^* V^* and T^*. In this paper we compare the characteristic pressure P^* of the mVW-EOS to the various pressures $P_X = \Delta H_X/\Delta V_X$ deduced from thermodynamic and kinetic properties of polymers in the liquid and solid states. ΔH_X and ΔV_X are: a) the enthalpy and volume change at the melting and glass transitions (the glass being isotropic or oriented and annealed below T_g at various aging conditions); b) the activation parameters of individual β and cooperative α motions in crystalline liquid and amorphous polymers studied by dielectric or mechanical spectroscopy; and c) the activation parameters of amorphous (solid and liquid) polymers submitted to a deformation depending on the time frequency temperature and strain rate. For a same material, whatever its state and whatever the experimental properties analyzed (dielectric and mechanical relaxation, viscosity, auto-diffusion, yielding under hydrostatic pressure), we demonstrate that $P_X = P^* = 1/\gamma\kappa$, ($\gamma$ Grüneisen parameter, κ compressibility). In all polymers and organic compounds (and water), these pressures, weakly dependent on T and P near T_g and T_m at low pressure are characteristic of the H-H inter-molecular interactions. It is shown that the two empirical Lawson and Keyes relations of the compensation law can be deduced from the mVW-EOS.

1 Introduction

The modified Van der Waals Equation of State (mVW-EOS)

We have shown, in Part I and II (refs. [1] and [2]), that polymers and molecular compounds in the glassy liquid and crystalline states verify the modified Van der Waals Equation of State (mVW-EOS),

$$V - V^* = (V_0 - V^*)\frac{P^*}{(P + P^*)} \quad \text{(mVW-EOS)}, \tag{1a}$$

which depends on the temperature via the volume $V_0(T)$ at zero pressure and on the characteristic parameters V^*T^* and P^*.

The zero-pressure bulk modulus B_0, its pressure derivative B_0' at $P = 0$, and the thermal pressure $(\mathrm{d}P/\mathrm{d}T)_V$ deduced from this EOS are:

$$B_0 = P^*\frac{V_0}{V_0 - V^*}, \qquad B_0' = \frac{V_0 + V^*}{V_0 - V^*},$$
$$B(P) \approx B_0 + B_0' P, \tag{1b}$$

$$\left(\frac{\mathrm{d}P}{\mathrm{d}T}\right)_V = B\,\alpha_V = P^*\frac{V_0'}{V - V^*} = \frac{P^* + P}{\Delta T^*},$$
$$\Delta T^* = T - T_0. \tag{1c}$$

The $P^*V^*T^*$ values are determined directly from the fit of the mVW-EOS with the PVT data at high pressure, and by various methods, such as the FST-Ist and FST-Isb (fan structure of the tangent to the isotherms and isobars).

a) *FST-Isb.* The tangents to the isobars $V(T)$ converge to the point V^*T^*. For glassy polymers the volume $V^*\alpha$ and $V^*\beta$ deduced from the mVW-EOS below and above T_g are very similar (13% difference, see table 2, Part I). The T^* values deduced from the FST properties of Glycerol OTP and Salol in the liquid state coincide exactly with the Vogel temperature T_0 deduced from the VFT law. In semi-crystalline polymers (polyethylene propylene and polyamide 6) the same property is observed (see tables 3 and 4, Part II). Then in relation (1c) the temperature derivative of the zero pressure volume is $V_0' = (V_0 - V^*)/(T - T_0)$.
b) *FST-Ist.* The tangents to the isotherms $V(P)$ at $P = 0$ converge to the point P^*V^*. The FST methods are described in Parts I and II. For a same material in the various states (glassy liquid or crystallized) the P^*V^*

---

[a] e-mail: `jacques.rault@yahoo.fr`

values determined by these methods coincide and are V T and P independent.

The bulk modulus, $B(P)$, extrapolates to zero at the negative pressure $P = -P^*$. Divergence of the compressibility $\kappa(P)$ in expanded solids and liquids near P^* cannot be determined experimentally, but only by extrapolating the PVT data obtained in compression ($P > 0$). As noted by Brosh *et al.* [3], the different EOS of Rose *et al.* [4] Baonza *et al.* [5] and Traravillo *et al.* [6] also predict a similar divergence of the compressibility for negative pressures (in the so-called spinodal, metastable region).

Anharmonicity and characteristic pressure P*

The anharmonicity of any material liquid or solid is characterized by the dimensionless Grüneisen parameter γ. Different forms of this parameter have been proposed and discussed in ref. [7] and in various text books (refs. [8,9]). Here we show that P^* can be deduced from the thermal γ_{th} and Slater-Grüneisen γ_{B} parameters. γ_{th} depends on the heat capacity C_P (or C_V) thermal expansion coefficient α and adiabatic (or isotherm) compressibility κ_S (or κ_T). γ_{B} depends on the pressure variation B' of the bulk modulus:

$$\gamma_{\mathrm{B}} \approx -\frac{1}{2}\frac{V(\mathrm{d}^2P/\mathrm{d}V^2)_T}{(\mathrm{d}P/\mathrm{d}V)_T} = -\frac{1}{2}B' - \frac{1}{2} \approx \frac{V_0}{V_0 - V^*}, \quad \text{Slater;} \tag{1d}$$

$$\gamma_{\mathrm{th}} = \frac{\alpha V}{C_P \kappa_S} = \frac{\alpha V}{C_V \kappa_T}, \quad \text{Grüneisen.} \tag{1e}$$

In most materials, α and C_V present variations with very similar to T, and the temperature variation of κ_T is negligible compared to those of α and C_V [9]. At low pressure ($P < P^*$) the temperature variation of the Slater-Grüneisen parameter deduced from the mVW-EOS, $\gamma_{\mathrm{B}} \sim V/(V - V_0) \sim T/(T - T_0)$, is negligible for $T > T_0$. Above the Debye temperature, around T_m and T_g the Slater and the thermal Grüneisen parameters are of the same order, $\gamma = \gamma_{\mathrm{th}} \sim \gamma_{\mathrm{B}}$. Thus, for $T \gg T_0$ the Grüneisen parameter will be considered as a constant.

The characteristic pressure P^* deduced from the VW-EOS is then, at low pressure,

$$P^* = \frac{2B_0}{B_0' + 1} = \frac{B_0}{\gamma} = \frac{1}{\gamma\kappa}. \tag{1f}$$

Typical values for polymers are $B_0 = 1/\kappa = 2.5\,\mathrm{GPa}$ and $\gamma_{\mathrm{B}} = 4$ to 7. See, for example, ref. [7]. The characteristic pressure P^* of polymer glass formers is around 0.4 GPa. For metals and mineral glasses $B_0 = 100$–$250\,\mathrm{GPa}$ and $\gamma_{\mathrm{B}} = 1.7$ to 2 [8,9], P^* is of the order of 50 to 100 GPa.

Here we do not compare the mVW-EOS to the various EOS given in the literature (more than 20; see, for example, references in Part I). We only want to compare this pressure P^* to other characteristic pressures deduced from crystallization (Clapeyron law), physical aging and rheology (the Eyring law and VFT law; viscosity diffusivity autodiffusion) and mechanical properties (modulus yield creep).

Generally the kinetic processes in liquids and solids follow the compensation law, so P^* will be compared to the characteristic pressure deduced from this empirical law.

The compensation law

The compensation law, Meyer-Neldel (MN) [10] or Lawson-Keyes (LK) [11–13] rule, is an empirical law known since 1937. An equivalent formulation, the isokinetics rule, has been known since 1929 by chemists. Many kinetic processes in liquid amorphous and crystalline materials are ruled by this law, such as annealing electronic trapping and conduction, chemical reactions, auto-diffusion, hetero-diffusion and yield stress. One will find references in the papers of Yelon *et al.* [14,15] Peakock-Lopez *et al.* [16] and Ngai [17]. These authors pointed out that the MN law, which states that the entropy and the activation energy and volume of the kinetics process are proportional, arises naturally in situations in which the activated energy for the process is considerably larger than both the thermal energy kT and the typical excitations of the system. This empirical law has been observed in a wide range of areas in chemical (and biological) reactions [18,19] in plasticized polymers [20–23] and in metals [24,25]. In refs. [7,26] we have interpreted the linear variations of the yield stress in polymer glasses with T and P in the framework of the compensation law and of the VFT law.

From the temperature and pressure dependence of such activated process, activation enthalpy ΔH energy ΔE, entropy ΔS and activation volume ΔV are measured. Various form of the Eyring equation exist. The simplest form is written as follows:

$$X = A(T, c)\exp -\Delta G/RT, \quad \Delta G = -T\Delta S + \Delta E + P\Delta V, \tag{2a}$$

$$\Delta H(p = 0) = \Delta E = R\,\mathrm{d}\ln X/\mathrm{d}(1/T), \quad \Delta V = RT\,\mathrm{d}\ln X/\mathrm{d}P. \tag{2b}$$

X is the relaxation time viscosity creep time, or the inverse of relaxation frequency, diffusivity, deformation rate.

In the following, ΔH is the activation enthalpy at ambient pressure (ΔE the activation energy at $P = 0$). The term A is often assumed to be T and lattice parameters (c) dependent, but this is not discussed here. Lawson [12,13] and Keyes [11] have shown that for diffusion of impurities in amorphous polymers the ratios $\Delta S/\Delta V$ and $\Delta V/\Delta H$, weakly dependent on the nature of impurities, do depend essentially on the nature of the host matrix (thermal expansion α and compressibility κ) according to the compensation rules, called here LK relations:

$$\Delta S = \frac{\alpha}{\kappa}\Delta V, \quad \Delta V = k\kappa_T\Delta H \quad \text{(LK relations).} \tag{3a}$$

Similar relations (with $k \sim 4$) have been observed in polymer glasses by Kowarskii [27].

Table 1. Thermal pressure of polymers and water in the melt state and of NaCl Fe in the crystalline state. Values deduced from the PVT properties above T_g or T_m in the temperature range ΔT.

Polymer	ΔT range (°C)	T_g (T_m) °C	$(\mathrm{d}P/\mathrm{d}T)_V$ MPa K^{-1}	Ref.
Natural rubber	20–50	−72	1.26	[27, 28]
Poly(dimethyl siloxane)	25–162	−133	0.79	″
Polyethylene high density	139–192	−20 (145)	1.21	″
Polyisobutylene	10–172	−73	1.16	″
Polyoxyethylene	50–103	−67 (80)	1.53	″
Polystyrene	27–100	100	1.42	″
Poly(vinyl methyl ether)	20–120	−31	1.28	″
Polysulfone	200–371	185	1.08	[29]
Water	40–140	(0)	1.6	[30]
NaCl	300–1050	(800)	2.8	[31]
ε-Fe	300–973	(1529)	6.8(±0.3)	[32]

The first LK relation, which is equivalent to the Maxwell relation, then from the mVW-EOS the thermal pressure coefficient $(\mathrm{d}P/\mathrm{d}T)_V$ at constant volume is obtained:

$$\left[\frac{\mathrm{d}P}{\mathrm{d}T}\right]_V = \left[\frac{\mathrm{d}S}{\mathrm{d}V}\right]_T = -\left[\frac{\mathrm{d}V}{\mathrm{d}T}\right]_P \Big/ \left[\frac{\mathrm{d}V}{\mathrm{d}P}\right]_T = \alpha B,$$

$$\left[\frac{\mathrm{d}P}{\mathrm{d}T}\right]_V = \frac{\alpha}{\kappa_T} \approx \frac{P^*}{T-T^*}; \quad P \ll P^*. \tag{3b}$$

The last relation at low pressure is the mVW-EOS relation (1c). As shown in Part I (tables 2, 3), the characteristic pressure T^* of crystallisable polymers (PE, PP, PA-6, PC, PCL) and organic compounds (Salol, Glycerol, OTP) is very near the Vogel temperature T_0. The T^* value of others polymers (atactic polymers such as PS PMMA PVAc) is about 100 °C below T_0.

The thermal pressure α/κ of polymers and water

One will find in ref. [27] (table 6, Chapt. 1) and in ref. [28] (table 7.7, p. 87) the temperature variation of the thermal pressure of various polymers; this parameter for various polymers is given in table 1; for comparison the thermal pressure of water, NaCl and Fe are also given. References are also given.

In polymers the thermal pressure is about 0.8 to 1.28 MPa/K, thus very similar to that of water (1.6 MPa/K). It must be noted that the cross-over temperature T_B (or T_m) of these polymers is about 150 °C above T_0 (typically: $T_g - T_0 = C_2 = 50\,^\circ\mathrm{C}$ and $T_B - T_g = 100\,^\circ\mathrm{C}$); P^* is of the order of 0.2 GPa. Relation (3b) gives the same value of the thermal pressure $\alpha/\kappa \sim 1$–$3\,\mathrm{MPa\,K^{-1}}$. It is important to note that the experimental and predicted temperature variations of this parameter are of the same order and can be neglected in a domain of 50 °C (variation of 5 to 15%). In glassy minerals this weak dependence of this thermal pressure with T was noted by some authors (see Part I); for example in NaCl, between 300 and 1050 K and for $P < 28\,\mathrm{GPa}$, Shanker *et al.* [31] found that $\alpha/\kappa \sim 2.8\,\mathrm{MPaK^{-1}}$ is nearly constant (only 10% variation) when α and κ vary by a factor 2 in the temperature domain ΔT and at low pressure $P < P^*$. In metals, Fe Cu Zn Cd, this parameter is between 5 and 7 MPa/K (see ref. [6] which gives α and κ of various metals and minerals); this is about one order of magnitude higher than those of polymers and water.

Kell *et al.* [30] and Fisher *et al.* [33] have studied the PVT properties of water at low pressure $0 < P < 0.1\,\mathrm{GPa}$ and between 40 and 140 °C. From the fan structure of the tangents to the $V(P)$ curves one finds that the convergent point coordinates are $V^* = 0.8\,\mathrm{cm^3/g}$ $P^* = 0.45 \pm 0.05\,\mathrm{GPa}$, the same values are deduced from the mVW-EOS fit with the experimental data (see table 2 of ref. [33]).

In polymers and water (above room temperature), the characteristic pressure P^* and the thermal pressure α/κ are very similar. One concludes that the variation of the volume with T and P in these materials is due essentially to the same intermolecular H-H Van der Waals interactions.

Origin of the compensation LK rules

As observed experimentally (see hereafter) the product $k\kappa$ is weakly dependent on T. Thus the temperature derivative of the second LK relation gives

$$\frac{\mathrm{d}V}{\mathrm{d}T} \approx k\,\kappa_T C P, \qquad k = \gamma_{\mathrm{th}} = \frac{\alpha V}{\kappa_T C_P}.$$

The constant k is then the thermal Grüneisen parameter $\gamma = \gamma_{\mathrm{th}} \sim \gamma_{\mathrm{B}}$. It is well known that γ is constant across the T_m and T_g transitions of crystalline metals and glassy polymers (see table A of ref. [34]). By integration, taking

Table 2. Melting enthalpy L_m and volume jump ΔV_m at the melting temperature T_{m0} of semi-crystalline polymers. Data come from tables II.2 and 4.12 of refs. [28] and [35]. P_{L_m} is the Clapeyron characteristic pressure (eq. (4)). P^* is deduced from the mVW-EOS. Polyethylene PE, Polypropylene PP, Poly4methylpentene P4MP, Polyoxyethylene PEO, Polyethyleneterephtalate PET.

	PE	PP	P4MP	PEO	PET
T_{m0} (K)	418	425	523	479	613
L_m (kJ/mol)	4.14	8.78	5.3	8.7	23.4
ΔV_m (cm^3/mol)	3.1–5.9	9.6	9.8	5.3	11.5–16.9
P_{L_m} (GPa)	1.3–0.7	0.9	0.5	1.6	2–1.4
P^* (GPa)	0.25	0.12			

into account eq. (1f), we conclude that

$$\Delta V = \gamma \kappa_T \Delta H, \qquad P_{H/V} = P^* = \frac{\Delta H}{\Delta V}. \tag{3c}$$

In conclusion, the two KL relations (the compensation rule, eq. (3a)) are consequences of the Grüneisen relation if one assumes that γ and κ can be considered as T and P independent (around the glass and melting temperatures and at low pressure, $P < P^*$).

For any thermodynamic (first-order transition) and kinetic process (aging, deformation, viscosity) a transition and activation enthalpy ΔH volume ΔV and then a characteristic pressure $P_{H/V} = \Delta H/\Delta V$ are determined. We analyze hereafter these properties in various solid and liquid polymers and organic compounds. We show that the pressure $P_{H/V}$ is equal to the characteristic pressure $P^* = 1/(\gamma\kappa)$ of the mVW-EOS (or not very different).

2 Crystallization: Enthalpy and volume change at T_m

2.1 Semi-crystalline polymers

The Clapeyron equation is written in the following form:

$$P_{T_m} = P_{L_m}, \quad P_{T_m} = T_{m0}\frac{\mathrm{d}P}{\mathrm{d}T_m}, \quad P_{L_m} = \frac{L_m}{\Delta V_m}. \tag{4}$$

P_{T_m} and P_{L_m}, called hereafter the characteristic Clapeyron pressures, are deduced from the melting temperature $T_{m0} = T_{m(P=0)}$ and its pressure variation $\mathrm{d}T_m/\mathrm{d}P$, from the latent heat $\Delta H_m = L_m$ and volume jump ΔV_m at the melting temperature T_{m0}.

In table 2 the characteristic pressures P_{L_m} of 5 semi-crystalline polymers are given, L_m and ΔV_m data come from table 4.12 of ref. [35] and table 11.2 of ref. [28]. The values of P_{L_m} are between 0.5 and 1.5 GPa. The uncertainty of the P_{L_m} value comes from the difficulties of measurement in materials with two different phases (liquid and crystalline). As noted in Part I (see tables 2 and 3) all polymers with H-H inter-molecular interactions have P^* values between 0.2 and 0.4 GPa, values obtained by PVT measurements in the liquid state. Taking into account the accuracy of the measurements in these semi-crystalline polymers and the uncertainty of the crystallinity we conclude that P_{L_m} and P^* are of the same order of magnitude.

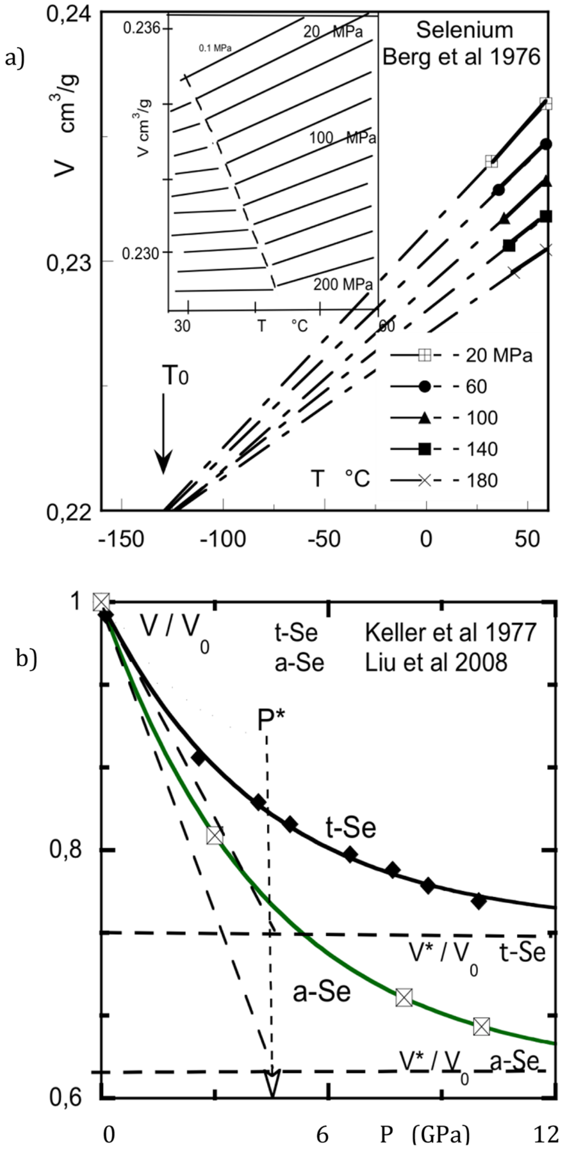

Fig. 1. Specific volume of selenium as a function of the temperature and pressure. (a) $V(T)$ data above the glass transition of Berg *et al.* [36] at 5 different pressures, in the insert schematic isobars in the liquid and amorphous states, steps 20 MPa up to 200 MPa. At the convergence point of the isobars the extrapolated temperature is the Vogel temperature. (b) Isotherms at ambient temperature of amorphous and crystalline Se. Data from refs. [38, 39].

2.2 Organic compounds and selenium

In Part I we have shown that the parameters $P^*V^*T^*$ can be found graphically from the FST to the isotherms and isobars in total agreement with the values obtained by the fit of the experimental P-V data with the mVW-EOS. As an example we apply these methods to the case of selenium which will be compared to three organic com-

Table 3. Characteristic temperatures of crystallisable glass formers. T_g glass temperature, T_0 Vogel temperature, T_m melting temperature at ambient temperature. Data from tables 2.9 and 2.11 of ref. [37]. P_{CP} pressure at the convergence point of the $T_g(P)$ and $T_m(P)$ curves. P^* characteristic pressure deduced from the mVW-EOS, table 3 of ref. [1]. $m^* P_{T_m}$ is the characteristic pressure given by eq. (5).

	T_g (K)	T_m (K)	T_0 (K)	m^*	$\mathrm{d}T_m/\mathrm{d}P$ (K/GPa)	P_{Tm} (GPa)	$m^* P_{T_m}$ (GPa)	$-P_{\mathrm{CP}}$ (GPa)	$P^*(EOS)$ (GPa)
Glycerol	189	290	126	0.56	66,5	4.4	2.4	3	(1–0.5)
OTP	241	329	168	0.49	366	1.14	0.55	0.3	0.25
Salol	219	317	175	0.45	277	1.02	0.45	0.3	0.2
Selenium	304	459	(160)	0.65	133	3.45	2.2	3	4.3

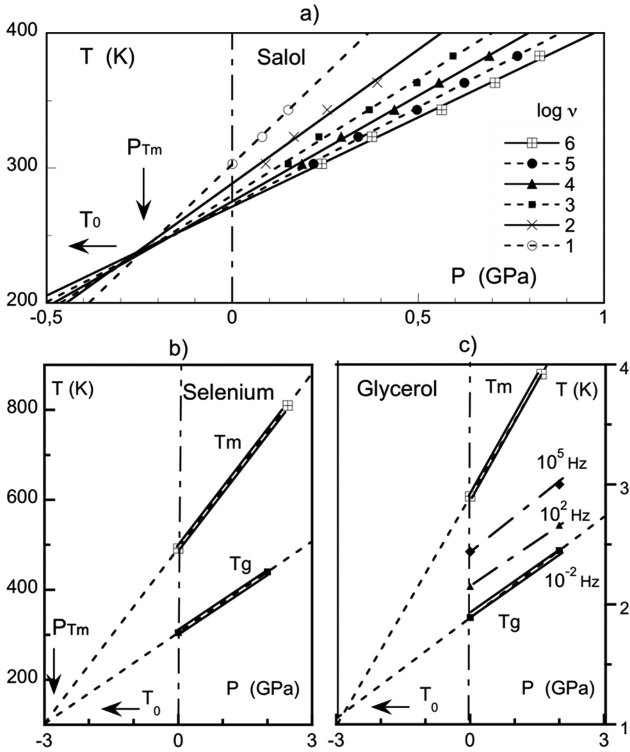

Fig. 2. Isochrone curves T *versus* P of liquids Salol, selenium and Glycerol, for different viscosity v (Poise) (a) and relaxation times or frequency (b, c). See references in the text and in ref. [2]. From the fan structure of the linear isochrone curves (FSIc) the Vogel temperature $T0$ and the characteristic pressure P_{T_m} are determined. References are given in Part I [1].

pounds. In fig. 1(a) we report the isobars $V(T)$ of Se, data from Berg *et al.* [36] between 30 and 60 °C. The fan structure of the isobars (FST-Isb) is clearly observed. The coordinates of the convergence point are: $T^* = 150\,\mathrm{K}$, $V^* = 0.22\,\mathrm{cm}^3/\mathrm{g}$. The T^* value is not far from the Vogel temperature $T_0 = 160\,\mathrm{K}$ reported by Donth [37]. In fig. 1(b) one sees that the P-V data at room temperature of tetragonal and amorphous Se of Keller *et al.* [38] and Liu *et al.* [39], the fits with the mVW-EOS (in plain lines) give the same characteristic pressure $P^* = 4.3\,\mathrm{GPa}$ and the same V^* value, although the initial volumes V_0 at $P = 0$ are different. The tangents to the isotherms at $P = 0$ intersect the horizontal lines V^*/V_0 at P^*. The parameters $P^* V^* T^*$ of the mVW-EOS are characteristic of the nature of the interactions and not on the state of the material (crystalline or liquid). In conclusion the properties of the mVW-EOS described for polymers (Part I) are also observed for selenium. The pressure variation of the glass and melting transitions of Se and of crystallizable organic compounds must be compared.

T_g and T_m transitions

In Part II (see fig. 11 and table 4 of ref. [2]) from the isotherms $\log\tau(P)$ of various crystallisable compounds we have deduced the isochrone curves $T(P)\tau$ or $P(T)\eta$ at constant relaxation time τ or viscosity η, the curves $T(P)\tau$ and $T(P)\eta$ of Salol selenium and Glycerol are reported in fig. 2, Orthoterphenyl (OTP) presents the same behavior, references are found in Part II for organic compounds and in the paper of Drozd-Rzoka *et al.* for selenium [40].

The fan structure of the tangent to the isochrones (FST-Isc) is observed in a large domain of temperature (50 to 100 °C below T_m). The important point to note is that the transition line, Clapeyron curve $T_m(P)$, is an isochrone (iso-viscosity) curve, this invariance of the dynamical properties of the liquid at T_m was noted by Fragiadakis *et al.* [41]. Analyzing the pressure dependence of the viscosity and melting temperature of metals Poirier [42] arrived at a similar conclusion. The coordinates of the convergence point of the FST-Isc at $P = 0$ ($P_{\mathrm{CP}}, T_{\mathrm{CP}}$) are not far from the mVW-EOS characteristic pressure P^* and the Vogel temperature T_0. See table 4 of ref. [2]. The relation between P_{CP} ($\sim P^*$) and P_{L_m} is then

$$\frac{T_m}{P_{L_m}} = \frac{\mathrm{d}T_m}{\mathrm{d}P} = \frac{T_m - T_0}{P_{\mathrm{CP}}}$$

$$m^* = \frac{T_m - T_0}{T_m}, \qquad P_{\mathrm{CP}} = m^* P_{T_m}. \tag{5}$$

In table 3 the characteristic temperatures, T_0, T_g, T_m, and the characteristic pressures, P_{CP}, P_{T_m}, P^*, of the four compounds are compared. The parameter m^*, describing the non-Arrhenius behavior of these crystallizable materials, is between 0.45 and 0.65.

The P^* value is deduced from the fit of the P-V data with the mVW-EOS (part I); for Glycerol the values in bracket are deduced from the FST to the $\log \eta(P)$ and $V(P)$ curves (fig. 6(a), (b)) of Part II). We conclude that eq. (5) is verified and the characteristic pressure P^* deduced from the mVW-EOS is equal to the pressure P_{CP} deduced from the isochrone curves $T(P)_\tau$.

3 Aging of glasses: Enthalpy and volume change at T_g

A glass annealed during the aging time t_a at T_a below the glass transition temperature T_g densifies. The kinetics of this process in isotropic polymers has been interpreted in the framework of the Vogel-Fulcher-Tamann (VFT) law [34, 43, 44]. In ref. [45] we have shown that the processes of aging in isotropic and oriented polymers are exactly similar. The physics of the first-order melting transition and of the kinetic T_g transition are obviously completely different but we notice here a very apparent intriguing similarity never noted up to now. By differential thermal calorimetry (DSC) and dilatometry under ambient pressure it has been found that the change of relaxation enthalpy volume and T_g (ΔH_{ag}, ΔV_{ag}, ΔT_{ag}) at constant heating rate vary linearly with $\log t_a$ between the incubation t_i and final t_f times. These times depending on T_a are deduced from the VFT law, and the relaxation parameters deduced from this law verify the relations

$$\Delta H_{ag} = k_H \log t_a/t_i,$$

$$\Delta V_{ag} = k_V \log t_a/t_i, \quad (t_i < t_a < t_f)$$

$$k_H = C_2 \Delta C_P/C_1, \qquad k_V = V C_2 \Delta\alpha/C_1. \qquad (6a)$$

C_1 and C_2 are the constant of the WLF law giving the relaxation time of the cooperative motions: $\log \tau/\tau_g = C_1(T - T_g)/(T - T_g + C_2)$. ΔC_P and $\Delta\alpha$ are the change of heat capacity and thermal expansion coefficient at T_g. The characteristic pressure P_{ag},

$$P_{ag} = \frac{\Delta H_{ag}}{\Delta V_{ag}} = \frac{\Delta C_P}{V \Delta\alpha}, \qquad (6b)$$

is then found to be independent of t_a and T_a and independent of the draw ratio in oriented polymers. P_{ag} is a characteristic parameter of the nature of the material as are the characteristic pressures P_{L_m} (and P_{T_m}) and P^*. In fig. 3 we report the typical DSC curves at constant heating rate of isotropic PS annealed at 85 °C (15 °C below T_g) for various times, from which the maximum and area of the peak of the subtracted curves ΔH_{ag} and T_{ag} are deduced. See refs. [34, 43]. The relaxation enthalpy volume and T_{ag} vary linearly with $\log t_a$ in a domain of 3 decades of aging time. As shown in [43] and [45] these aging properties of PS are also observed in others polymers (isotropic or oriented) annealed below T_g. The scaling relation $\Delta H_{\max} \sim \Delta T_{\max}$ recalls the linear relation $L_m \sim T_m$ of the crystalline materials (called the Nachtrieb rule [46]) and the relation $\Delta H_{ag} \sim \Delta V_{ag}$ is equivalent to the compensation LK relation, eq. (3c). For PS one finds that the characteristic pressure P_{ag} is of the order of 0.7 GPa, which is not far from the mVW-EOS pressure $P^* \sim 0.3$ GPa. In all polymers P_{ag} values are of the same order. One recalls that in Part I (and above in table 1) we have shown that the P^* values (and $(\mathrm{d}P/\mathrm{d}T)_V$ values) of polymers with H-H inter-molecular interactions are of the same order.

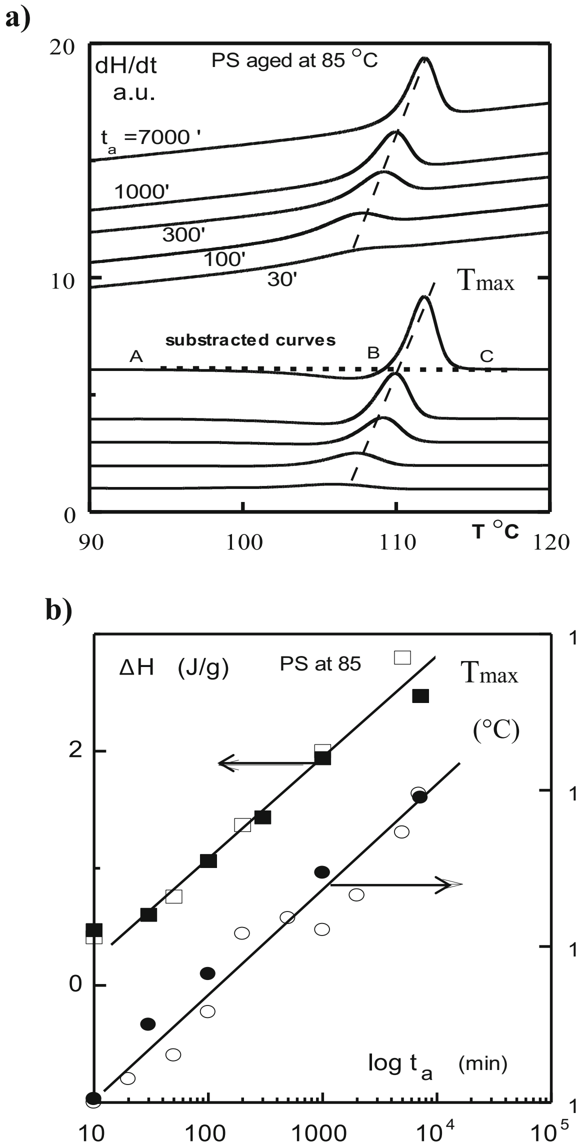

Fig. 3. Enthalpy relaxation of glassy PS aged at 85 °C during different times t_a. (a) Upper curves, DSC heat flow, $J = \mathrm{d}H/\mathrm{d}t$, *versus* temperature. Heating rate $q = 10\,°\mathrm{C/min}$. By subtracting the reference curve (no annealing) one obtains the lower curves. (b) Relaxation enthalpy ΔH and temperature $T_{\max}$ (at the maximum of the peak) as a function of the logarithm of aging time t_a. Filled symbols: isotropic PS. Open symbols: oriented PS [34, 43].

Relation with the Grüneisen relation

Assuming that the adiabatic compressibility κ_S varies weakly with the aging time t_a. The change of capacity ΔC_P and thermal expansion $\Delta\alpha$ during aging is given by the Grüneisen equation (1e)

$$\Delta C_P(t_a) = \Delta\alpha V \frac{1}{\kappa_S \gamma_{\text{th}}} = \frac{1}{\kappa_S \gamma_{\text{th}}} \mathrm{d}V(t_a)/\mathrm{d}T. \tag{6c}$$

As noted above, the T variation of the product $\gamma\kappa$ is considered negligible compared to those of V and C_P. Then, by integration,

$$\Delta H_{ag} = \int_{t_0}^{t_a} (C_P(t_0) - C_P(t_a))\mathrm{d}T,$$
$$\frac{\Delta H_{ag}}{\Delta V_{ag}} = \frac{1}{\kappa_S \gamma_{\text{th}}} = P^*. \tag{6d}$$

Equation (6d), which is the KL compensation relation, recalls the Clapeyron relation, all characteristic pressures, P_{T_m}, P_{ag} and P^*, are of the same order. The assumption $\kappa_S \gamma_{\text{th}} = \text{const.}$ leads to the equality $P_{ag} = P^*$; to explain the small difference between the experimental values of these two characteristic pressures P_{ag} and P^* (factor 2) it would be necessary to study the variation of κ_S as a function of the density (of the aging time) by measuring the temperature change caused by changing pressure under adiabatic conditions. It is well known that this method provides a direct determination of the product $\kappa_S \gamma$ [9], according to the thermodynamic relation $(\mathrm{d}T/\mathrm{d}P)_S = \kappa_S \gamma_{\text{th}} T$.

4 Liquids and solids: Activation enthalpy entropy and volume

4.1 Organic and polymer materials: The α and β transitions

By dielectric spectroscopy the mobility of the polar groups of polymers and molecular materials have been studied extensively. See refs. [27,47,48]. The viscosity η, and the relaxation time τ, of the supercooled liquid ($T_g < T < T_B$) follows the VFT m-VFT and WLF relations:

$$\eta \approx \tau = \tau_0 \exp \frac{B}{T - T_0} \quad \text{(VFT)},$$
$$\log \frac{\tau}{\tau_g} = C_1 \frac{T - T_g}{T - T_g + C_2} \quad \text{(WLF)}, \tag{7a}$$
$$\eta \approx \tau = \tau_0 \exp \frac{E_\beta}{n_s RT},$$
$$n_s(T) \approx n(T) = \frac{T - T_0}{T_B - T_0}, \quad T_g < T < T_B \quad \text{(m-VFT)}. \tag{7b}$$

In the framework of the sm-VFT model [2] the Kohlrausch exponent $n_S(T, P)$ is a sigmoidal function of T (often called the logistic function) depending on T_0, the Vogel temperature, and T_B, the bifurcation or cross-over temperature (in semi-crystalline materials $T_B = T_m$). In that case, eq. (7b) fits the experimental data in the entire experimental domain of temperature, α domain ($T_g < T < T_B$) and β domain (Arrhenius, $T > T_B$). See figs. 2–5 of ref. [2], for Benzyl Chloride (BC) Orthoterphenyl (OTP) Phenolphtalein dimethyl ether (PDE) and B_2O_3. For this last mineral glass the fit domain is $500 < T < 1700\,\mathrm{K}$ $T_g = 500\,\mathrm{K}$ and $T_B = 950\,\mathrm{K}$.

Table 4. Activation volume and energy of the individual (β) and collective (α) motions of three amorphous polymers. Data from ref. [27]. P_α and P_β are the characteristic pressures $\Delta H/\Delta V$ of the α and β motions.

	Process	$\Delta V = V_{\alpha,\beta}$ (cm^3/mol)	$\Delta H = E_{\alpha,\beta}$ (kJ/mol)	P_α, P_β (GPa)
PVC	α	321	525	1.6
	β	25	63	2.5
PMMA	α	398	355	0.9
	β	53	88	1.6
PET	α	518	880	1.7
	β	35	63	1.8

Between T_g and T_m (or) $n_S(T)$ can be approximated by a linear function of T which extrapolates to 0 at the Vogel temperature T_0 and to 1 at T_B; this is the modified VFT model (m-VFT).

In table 2.1 of ref. [47], one verifies that the activation energies E_β of the β transition is equal to E_η the activation energy of the viscosity (Newtonian viscous flow). The activation parameters, E_α, E_β, V_α, V_β, of the individual (β) and cooperative (α) motions in the melt at equilibrium vary very similarly with T and P. In refs. [2,7], we have shown that the relation between these parameters measured by various methods (on various organic materials and polymers) is

$$n = E^*_\beta / E^*_\alpha = V^*_\beta / V^*_\alpha. \tag{8a}$$

The Kohlrausch exponent n varies linearly with T between T_g and the cross-over temperature T_B (T_m in crystallizable materials), then the ratios $P_\alpha = E_\alpha/V_\alpha$ and $P_\beta = E_\beta/V_\beta$ are constant when T is changed as predicted by the compensation law (the empirical LK relation). The characteristic pressure $P_{\alpha,\beta}$,

$$P_\alpha = P_\beta = E_\beta/V_\beta = E_\alpha/V_\alpha, \tag{8b}$$

is T and P independent, as is the characteristic pressure P^* of the mVW-EOS (above T_g and at low pressure $P < P^*$).

In table 4 the activation parameters of three amorphous polymers are compared. The data come from the Kovarskii book. See tables 7 and 9, Chapt. 4 of ref. [27]. The measurements are done by dielectric spectroscopy at different temperatures. The P_α and P_β values of these polymers are given in the last column. The estimated accuracy is $\Delta P \sim 0.2\,\mathrm{GPa}$.

As noted above, the activation parameters of the α relaxation near T_g is about 10 times those of the β relaxation. One verifies the relation $P_\alpha \sim P_\beta$. The $P_{\alpha,\beta}$ values of the order of 0.8 to 1.6 GPa are about the P_{L_m} values (0.5 to 1.8) of semi-crystalline polymers (see table 2) and about 2 to 3 times the P^* values of amorphous polymers (see table 2 Part I). The accuracy of measurements on ΔV and ΔH have not been discussed by the authors quoted by Kovarskii. This author reports data obtained by various techniques and in various temperature domains. In table 7 of ref. [27] the activation values for a same polymer can present differences of 20 to 30% according to the authors. Taking into account the accuracy of the measurements we conclude that eq. (8b) is well verified. The ratio P_α/P_β is between 1 and 1.6 whereas the ratio E_α/E_β is of the order of 10.

4.2 Plastic flow of glassy polymers at ambient pressure: Creep and yielding

a) Upper yield stress

During deformation $\varepsilon(t)$ of a polymer glass at constant rate ε' the stress $\sigma(\varepsilon)$ increases, presenting at ε_y a maximum σ_y, called the upper yield stress, then decreases and levels off during the steady deformation (creep). The stress at the plateau is called the lower yield stress (or the flow stress). In fig. 4(a), the material has been quenched (t_1) and annealed during time t_a (t_2, t_3) at T_a below T_g. By DSC the difference in enthalpy between the annealed sample (t_2) and the quenched one (t_1) can be measured. This corresponds to the difference in mechanical energy during the two tests (dashed area in the figure). The difference of enthalpy ΔH and of upper yield stress, $\sigma_y = \sigma_{yl} + \Delta\sigma$, between the aged and not aged samples have been measured by several authors, as a function of aging temperature T_a and time t_a. In fig. 4(b) we report ΔH *versus* $\Delta\sigma$ for polycarbonate (PC) annealed at three temperatures and various times (data from Bauwens *et al.* [49]). It is clear that the characteristic volume $\Delta V = \Delta H/\Delta\sigma$ is constant, independent of t_a and T_a. The same linear plots are obtained for others cross-linked polymers (PEEK and DGEBA); the data come from refs. [50,51]. During aging below T_g the glass density increases (eq. (6a)). From similar changes of volume and enthalpy with aging time, $\Delta V \sim \Delta H \sim \log t_a$, one concludes that the ratio $\Delta H/\Delta V$ is constant (not dependent on aging conditions, t_a and T_a); this is the compensation LK relation.

Bauwens *et al.* [52] and Pink *et al.* [53] have studied in detail the dependence of the shear yield stress σ_y of PVC with temperature at strain rate $\varepsilon' = 3.4\ 10^{-4}\,\mathrm{s}^{-1}$. From these data, using a model of cooperative movement, Povolo *et al.* [54] have shown that the activation parameters ΔH and ΔV are linear functions of σ_y in the domain $20 < \sigma_y$ (MPa) < 70. From figs. 7 and 8 of this reference we conclude that the activation parameters of PVC at this strain rate verify the relations

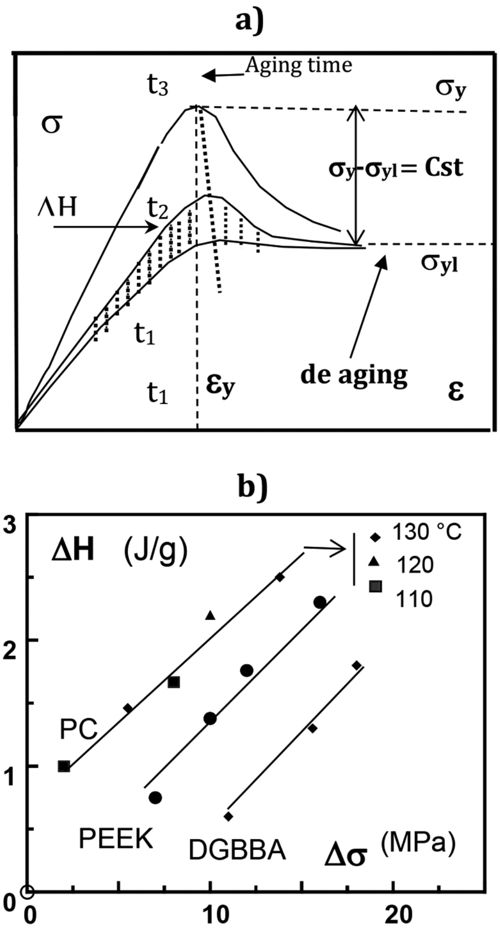

Fig. 4. (a) Stress strain curve $\sigma(\varepsilon)$ at constant strain rate ε' of a glassy material annealed during 3 different times below T_g. The upper σ_y and the lower σ_{yl} yield stresses are indicated. The dashed area is the mechanical energy to rejuvenate the aged material. (b) Enthalpy measured by DSC as a function of $\sigma_y - \sigma_{yl}$. The 3 glassy polymers have been annealed below T_g at different annealing temperatures and times [50–54]. PC polycarbonate, PEEK polyetherethercetone, DGBA epoxy resin.

$$\begin{aligned} \Delta H &= \Delta H_0(1 - \sigma_y/\sigma^*), \\ \Delta V &= \Delta V_0(1 - \sigma_y/\sigma^*), \qquad \sigma^* = 130\,\mathrm{MPa}, \\ P_{H/V} &= \frac{\Delta H}{\Delta V} = 0.2\ (\mathrm{GPa}). \end{aligned} \tag{9}$$

The characteristic pressure $P_{H/V} = 0.2\,\mathrm{GPa}$, independent of σ_y and T, is about the value of P^* of all the polymers analyzed in Part I (values between 0.2 and 0.38 GPa).

In conclusion, at ambient pressure, the characteristic pressure $P_{H/V}$ of polymers deduced from the upper yield stress is constant, independent of the aging conditions and of the order of the P^* value deduced from the mVW-EOS.

b) Lower yield stress

Nanzai *et al.* [55–58] have analyzed in detail the plastic flow (tension and compression) of various glassy polymers

Table 5. Characteristic pressure $P_{H/V}$ and compensation temperature T_C of polymers deduced from plastic flow (lower yield stress) below T_g. P^* is deduced from the mVW-EOS. Activation parameters come from Nanzai *et al.* [55–58], in bracket from Lefevre *et al.* [59]. PMMA polymethylmethacrylate, PVC polyvinylchloride, SAN styreneacrylonitrile, PC polycarbonate, PS polystyrene.

	PMMA	PVC	SAN	PC	PS
P^* (GPa)	0.38			0.19	0.26
$P_{H/V} = \Delta H/\Delta V$ (GPa)	0.1	0.13	0.46	0.12–(0.21)	0.33
$T_C = \Delta H/\Delta S$ (K)	394	341	393	344	370
T_g (K)	373	350	373–398	423	374

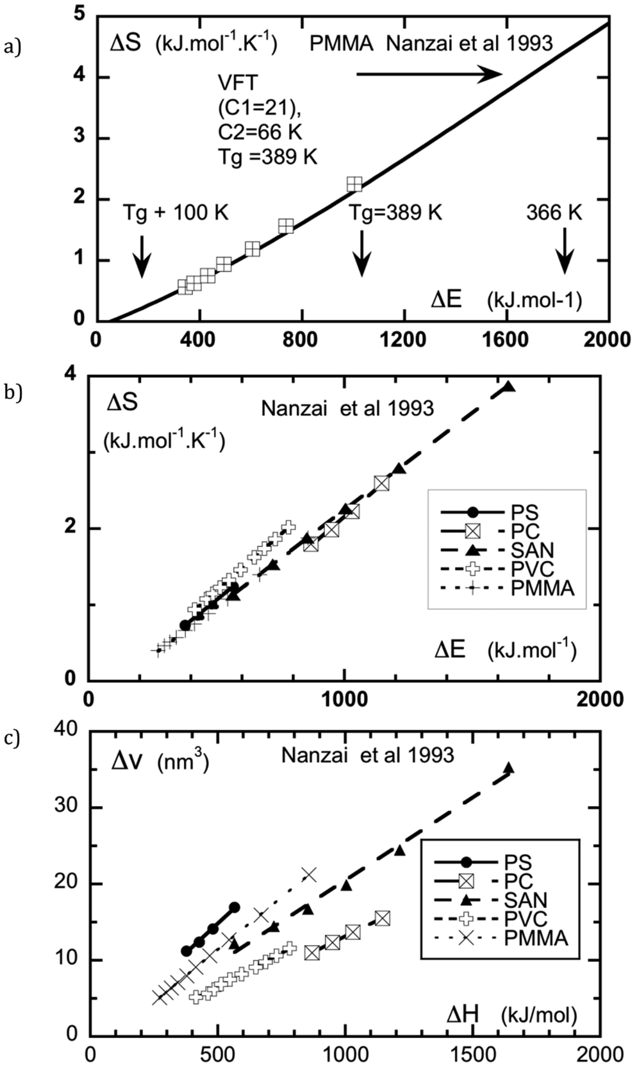

Fig. 5. Compensation plots of various glassy polymers. The activation parameters ($\Delta S, \Delta E, \Delta V$) are deduced from the temperature and pressure variations of the lower yield stress below T_g. Data from Nanzai *et al.* [55–58]. (a) PMMA, the heavy line is the prediction of the VFT law, eqs. (16.c) and (16.d). (b, c) Heavy lines are linear regression, the compensation law (KL rule) is observed. See text.

as function of the true strain rate ε' and the lower yield stress σ_y in a temperature domain of 20 to 50 °C below T_g, One recalls that the lower yield stress σ_{yl} is not dependent on the thermo-mechanical history of the material, thus not dependent on the aging of the glass below T_g. The compensation plots of these polymers are given in fig. 5. One verifies that the activation parameters, ΔH, ΔV, ΔS, are proportional. See tables 1–5 of refs. [55, 56] and table 1 of refs. [57, 58]. In fig. 5(a) the heavy line is the fit with the VFT law, see fig. 6 of ref. [7]. The compensation LK relations are observed above and below T_g. This was noted by Nanzai. The characteristic pressures $P_{H/V}$ and the compensation temperatures T_C deduced from these plots are given in table 5.

Nanzai *et al.* have compared the steady plastic flow of PC (at constant ε') in compression and tension. From the activation parameters given in table 1 of ref. [58] one notes that $P_{E/V} = \Delta H/\Delta V$ decreases by a factor 1.09 when ΔH (along with ΔV) increases by a factor 1.6, in both types of deformation. Then $P_{H/V}$ is considered as constant. The important point to note is that in tension and compression the characteristic pressures $P_{H/V}$ are equal: $P_{H/V} \sim 0.12\,\text{GPa}$.

In conclusion, during yielding at ambient pressure:

a) The three activation parameters, ΔH, ΔS, ΔV, are proportional when ε' and T change. The compensation LK relations are verified.

b) P^* and $P_{H/V}$ are of the same order, P and T independent; this is the LK relation.

c) $P_{H/V}$ has the same value in tension and compression, as is expected from the properties of the characteristic pressure P^*. The mVW-EOS is assumed to be valid in negative pressure.

d) The compensation temperature T_C and the glass transition T_g (measured at 10 °C/min by DSC) are of the same order, the experimental temperature domain being between 20 and 50 °C below T_g.

4.3 Plastic flow and modulus of polymers under hydrostatic pressure

It is well known that the modulus E and the yield stress σ_y of crystalline materials in uniaxial and shear deformation are proportional. In solid metals various theoretical models predict that $E/\sigma_y = 6$. In polymer glasses [27] and amorphous metallic alloys [60] the E/σ_y values are about 10 and 30. The effect of hydrostatic pressure on polymers is well known: E and σ_y vary linearly with T and P ($0 < P < 0.8\,\text{GPa}$). It has been shown in ref. [26]

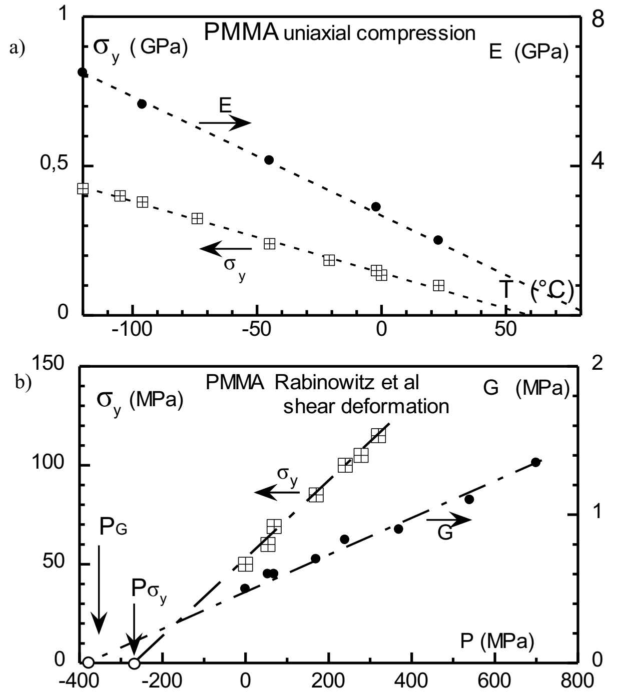

Fig. 6. Uniaxial (a) and shear (b) deformation of PMMA at constant deformation rate. Yield stress σ_y tensile and shear modulus E-G as a function of temperature (a) [61] and at room temperature as a function of the hydrostatic pressure (b) [62].

that the compensation law leads to the linear relations with T and P at constant strain rate ε':

$$\sigma_y = a(T_g - T), \quad a = \mathrm{d}\sigma_y/\mathrm{d}T, \tag{10a}$$

$$\sigma_y = \sigma_0(1 + P/P_\sigma), \quad P_\sigma = (T_g - T)\mathrm{d}P/\mathrm{d}T_g. \tag{10b}$$

At constant pressure (eq. (10a)) and at constant temperature (eq. (10b)), these relations are well verified, the constant a and σ_0 are dependent on ε'. See, for example, refs. [26, 27, 34]. Equation (10b) is the so-called *soil mechanic equation*, or the Mohr-Coulomb criterion. The tensile compressive and shear modulus (E, G) verify similar linear equations.

$$G \approx E = b(T_g - T), \quad b = \mathrm{d}E/\mathrm{d}T, \tag{11a}$$

$$G \approx E = E_0(1 + P/P_E), \quad P_E = (T_g - T)\mathrm{d}P/\mathrm{d}T_g. \tag{11b}$$

In fig. 6(a) we have reported the T dependence of E and σ_y of glassy PMMA at ambient pressure. For Bowden's data, see figs. 9 and 10 Chapt. 5 of ref. [61]. Equations (10a)–(11a) are verified in a large temperature domain ΔT below T_g ($\Delta T = 140\,^\circ\mathrm{C}$). The ratio E/σ_y is constant ~ 10 and both parameters extrapolate to zero a temperature near $T_g \sim 100\,^\circ\mathrm{C}$.

In figs. 6(b) and 7(a), (b), the pressure variations of E, G and σ_y of PMMA PC and PE in tension at ambient temperature are compared. The data come from the work of Rabinowitz *et al.* [62], Sauer *et al.* [63] and Tsirule *et al.* [64]. See also [27]. In a large domain of pressure ($0 < P < 0.6\,\mathrm{GPa}$) the above linear relations are σ verified. We have reported in table 6 the extrapolated values P_E and P_σ deduced from the P dependence of the flow stress and modulus. It is clear that these two characteristic pressures, P_σ and P_E, are equal. The accuracy of these extrapolated pressures is estimated to be important (20%). For PE and PMMA one verifies that these pressures are equal to P^* (values determined in Part I). This confirms that for the negative hydrostatic pressure,

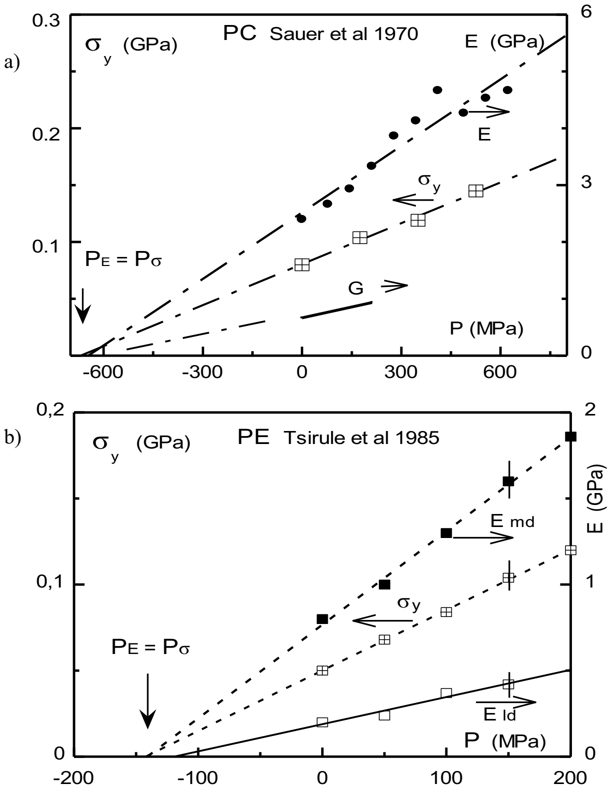

Fig. 7. Yield stress σ_y and modulus E of PC (a) and PE (b) in tensile deformation, at constant deformation rate and at room temperature, as a function of the hydrostatic pressure. In (a) G is the shear modulus, in (b) E_{md} and E_{ld} are tensile modulus of middle (md) and low (ld) density PE. See references in text.

Table 6. Characteristic pressures P_σ and P_E of 5 polymers and an alkali metal K under hydrostatic pressure deduced from the stress-strain curves. P^* is the characteristic pressure deduced from the mVW-EOS. Polymers: polyoxymethylene POM; polymethylmethacrylate PMMA; polycarbonate PC; polyimide PI; polyethylene PE.

(GPa)	P_E	P_σ	P^*_{EOS}	Ref.
POM	0.35	0.35		fig. 11 [64]
PMMA	0.40	0.30	0.38	fig. 14″
PC	0.68	0.80	0.19	fig. 19″
PI	0.25	0.13		fig. 20″
PE	0.15	0.15	0.26	fig. 22″
K	1.24	1.4	1.7	fig. 5 [67]

$P = -P^*$, the compressibility becomes infinite as predicted by the mVW-EOS. However we note, in table 6, a greater difference between the P^* value of PC (0.2 GPa see part I) and the P_E and P_σ values (0.67 and 0.8 GPa). One wonders whether this difference is due to the inaccuracy of the measurements or to a more physical reason.

In the review paper of Hoppel [65] one finds a comparison of the yield stress and modulus of polymers under hydrostatic pressure in vartious tests (compression, tension, shear). The E, G and σ_y values and their derivative depend obviously on the nature of the test, but the P_σ values deduced from these data are very similar to the values given in table 6 (and weakly dependent on the nature of the test).

Spitzig *et al.* [66] have compared the P dependence of the flow stress and modulus of PE and PC in tension and compression. Linear variations are observed up to 1 GPa. The characteristic pressures are equal $P_\sigma = P_E$, 0.2 and 0.8 GPa for PE and PC. These values are in perfect agreement with data with the others authors and with the P^* values of polymers deduced from the mVW-EOS. See Part I.

In table 6 we have also reported the P_σ and P_E values of potassium, deduced from the linear variations of E and σ with P (data of Chua *et al.* [67] at room temperature at 0, 3, 5.15 kbar). A good agreement between the P^* and P_σ values is again observed (values one order higher than those of polymers).

In conclusion, for all the materials analysed here the three characteristic pressures P_σ, P_E and P^* are equal (or not very different). It is important to verify this correlation for other materials, including metals and mineral compounds.

4.4 Relation between diffusion in melt and solid

As noted above, one will find, in the book by Bershtein and Egorov (tables 2.1–2.4, of ref. [47]), the properties of the cooperative α and individual β relaxations of various polymers (semi-crystalline and amorphous). The β motions observed by dielectric and mechanical spectroscopy have a constant activation energy (Arrhenius behavior) in the whole domain of temperature, in the glassy liquid and crystalline states, above and below the merging temperature T_B (or T_m for crystalline polymers). These authors give the activation energies of the viscosity Q_η in the liquid state and of the β motions E_β in the solid or liquid states of 12 polymers. All these energies are of the same order, between 30 and 100 kJ/mol. The accuracy is about 10%. The relation $Q_\eta = E_\beta$ is verified with very good accuracy (correlation factor $R_c = 0.95$). These authors also report the shear activation volume V_β of the β relaxation of 5 polymers (PC, PE, PMMA, PS, PVC) values 0.6 and 1.2 nm^3. The relation

$$P_{Q/V} = \frac{Q_\eta}{V_\beta} = \frac{E_\beta}{V_\beta} \qquad (12)$$

is verified. The pressure $P_{Q/V}$ characteristic of the liquid state (viscosity at T_B) is equal to the pressure P_β characteristic of the individual motions in the solid and liquid states. These pressures are equal to $P_{H/V}$ deduced from the work of Nanzai *et al.* [55–57] and to P^* deduced from the mVW-EOS (see table 5 and Part I).

Metallic glasses (multi-components alloys) present also the so-called secondary β transition below the α transition, $T_g > T_\beta > 0.7T_g$. By mechanical spectroscopy on various glassy alloys, Yu *et al.* [68] have studied the correlation between the β secondary relaxation and the self-diffusion of the smallest constituting atoms. They found that the activation energies of the β process E_β and of the self-diffusion Q_{sd} are equal. It would be interesting to study these alloys under pressure to verify (as in polymers) that the activation volumes of both process are also equal. Is the relation $P_{Q_{sd}} = P_\beta = P^*$ observed in these metallic glasses?

5 Conclusion and perspectives

Cooperative and local processes of transformation and deformation of any material imply a change of energy (latent heat, activation energy) volume (specific volume jump, activation volume) and entropy. The LK relations (of the so-called compensation law) are always observed. The changes of the properties of any polymer or organic compounds due to a change of temperature (melting of crystals, enthalpy and volume relaxation of aged glass) and of stress (yielding, viscosity) imply different ΔH and ΔV values but the ratio for a same material, $\Delta H/\Delta V = P_X$, is independent of T and P (near T_g and T_m for small pressure), whatever the physical process analyzed. These various pressures P_X ($P_{H/V}$, P_α, P_β, P_{ag}, $P_{Q/V}$) have been compared to the characteristic pressure P^* of the mVW-EOS. All these pressures are equal and T, P independent. The relations $P_{T_m} = P_{H/V} = P_{ag} = P_\sigma = P_Q$ and $P_X \sim P^*$ confirm the universal character of the modified Van der Waals law (mVW-EOS) and of the compensation law. The compensation LK relation $\Delta V = \gamma\kappa\Delta H$ (eq. (3a)), is then equivalent to the mVW-EOS relation, $P^* = B_{0/\gamma} = 1/\gamma\kappa$ (eq. (1e)). The given form of the two LK relations implies that the Grüneisen parameter and the compressibility are weakly dependent on T. This is generally observed [8,9]. This equivalence between P^* and the various characteristic pressures P_i determined in this work leads to various questions:

a) In many compounds the ratio P^*/P_X is about 1 to 1.4 (PMMA, PC, PS, Se) and, in other compounds, about 4 to 8 (for example $P^*/P_{Lm} \sim 4$ and 8 for PE and PP). One wonders if the high value of this ratio observed for a few compounds is due to the inaccuracy of the measurements, or to a systematic error in the process of the experiments (P and T calibration, sample preparation, or the presence of the plasticizer).
b) For any material, P^* and $P_{H/V}$ have the same values in liquid and solid states. Is the relation $P^* = P_{H/V}$ still valid in two different crystalline phases of the same material?
c) In a material presenting different crystalline phases separated in the phase diagram by the transition

line $T_{tr}(P)$ what is the Clapeyron pressure $P_{tr} = \Delta H_{tr}/\Delta V_{tr}$ (or $T_{tr}\mathrm{d}P/\mathrm{d}T_{tr}$) compared to the P^* values determined in the different crystalline phases?

d) Various materials present negative slope of the transition line $T_m(P)$, cerium, plutonium, germanium, bismuth, ice, etc. In cerium, δ, and plutonium, ε, it is found that the activation volume is negative [24]. In such crystalline elements and compounds what are the P^* values compared to the various characteristic pressures P_D, P_E and $P_{\sigma y}$ deduced by auto-diffusion modulus and yield stress measurements?

e) The relation between the compensation law and the equation of state (mVW-EOS) has been discussed here only in the case of small pressure ($P < P^*$). It would be interesting to study in detail the variations of the parameters C_P, α and κ of the different phases, liquid and solid, as functions of T at high pressure. Is the Grüneisen parameter γ still constant at high pressure?

In our next paper we will show that the relations between the characteristics pressures, P^*, $P_{H/V}$ and P_{T_m}, observed in amorphous and semi-crystalline polymers are also observed in other crystalline materials: simple mineral and metallic elements, oxide and halide compounds.

References

1. J. Rault, Eur. Phys. J. E **37**, 113 (2014).
2. J. Rault, Eur. Phys. J. E **38**, 91 (2015).
3. E. Brosh, G. Makov, R.Z. Shneck, J. Phys.: Condens. Matter **15**, 2991 (2003).
4. J.H. Rose, J. Smith, F. Guinea, J. Ferrante, Phys. Rev. B **29**, 2963 (1984).
5. V.G. Baonza, M. Céceres, J. Nünez, Phys. Rev. B **51**, 28 (1995).
6. M. Taravillo, M. Baonza, V.G. Nunez, M. Caceres, High Temp. High Pressure **30**, 97 (1998).
7. J. Rault, Eur. Phys. J. E **35**, 26 (2012).
8. J.C. Slater, *Introduction to Chemical Physics* (McGraw-Hill, New York, 1939).
9. T.H.K. Barron, G.K. White, *Heat Capacity and Thermal Expansion at Low Pressure* (Kluker Academic, New York, 1999).
10. W. Meyer, H. Neldel, Z. Tech. Phys. **12**, 588 (1937).
11. R.W. Keyes, J. Chem. Phys. **29**, 467 (1958).
12. A.W. Lawson, J. Phys. Solids **3**, 250 (1957).
13. A.W. Lawson, J. Chem. Phys. **32**, 131 (1960).
14. A. Yelon, B. Movagha, Phys. Rev. Lett. **65**, 618 (1960).
15. A. Yelon, B. Movagha, H.M. Branz, Phys. Rev. B **46**, 12244 (1992).
16. E. Peacock-Lopez, H. Suhl, Phys. Rev. B **26**, 3774 (1982).
17. K.L. Ngai, Solid State Ionics **105**, 23 (1998).
18. K.F. Freed, J. Phys. Chem. B **115**, 1689 (2011).
19. L. Liu, Q.-X. Guo, Chem. Rev. **101**, 673 (2001).
20. T. Psurek, C.L. Soles, K.A. Page, M.T. Marcus, T. Cicerone, J.F. Douglas, J. Phys. Chem. B **112**, 15980 (2008).
21. A. Anopchenko, T. Psurek, V. VanderHart, J.F. Douglas, J. Obbrzut, Phys. Rev. E **74**, 031501 (2006).
22. Y. Hiki, H. Takahashi, H. Kobayashi, Solid State Ionics **53-56**, 1157 (1992).
23. Y. Hiki, J. Non-Cryst. Solids **357**, 357 (2011).
24. Y. Adda, J. Philibert, *La diffusion dans les solides* (Presses Universitaires, 1966).
25. J. Philibert, Trans. Tech. Publ. **249**, 61 (2006).
26. J. Rault, J. Non-Cryst. Solids **235-237**, 737 (1998).
27. A.L. Kovarskii, *High-Pressure Chemistry and Physics of Polymers* (CRC Press, Boca Raton, 1993).
28. J.E. Mark (Editor), *Physical Properties of Polymers Handbook* (AIP Press, NY, 1995).
29. P. Zoller, J. Polym. Sci.: Polym. Phys. **16**, 1261 (1978).
30. Kell Whalley, J. Chem. Phys. **62**, 1063 (2008).
31. J. Shanker, M. Kumar, Phys. Status Solidi B **179**, 351 (1993).
32. T. Uchida, Y. Wang, M.L. Rivers, S.R. Sutton, J. Geophys. Res. B **106**, 21799 (2001).
33. F.H. Fisher, O.E. Dial, *Equation of State of Pure and Sea Water*, Rep. SIO reference 75-28.
34. J. Rault, *Physical Aging of Glasses: the VFT approach* (Nova Science Publishers, New York, 2009).
35. D.W. Van Krevelen, *Properties of Polymers* (Elsevier, Amsterdam, 1990).
36. J.I. Berg, R. Simha, J. Non-Cryst. Solids **22**, 1 (1976).
37. E. Donth, *The Glass Transition* (Springer, Berlin, 2001).
38. R. Keller, W.B. Holzapfel, H. Schulz, Phys. Rev. **16**, 1403 (1977).
39. H. Liu, L. Wang, X. Xiao, F. De Carlo, J. Feng, H. Mao, R. Hemley, Proc. Natl. Acad. Sci. U.S.A. **105**, 13229 (2008).
40. A. Drozd-Rzoska, S.J. Rzoska, A.R. Imre, J. Non-Cryst. Solids **353**, 3915 (2007).
41. D. Fragiadakis, M.C. Roland, J. Phys. Rev. E **83**, 031504 (2011).
42. J.P. Poirier, Geophys. J. **92**, 99 (1988).
43. J. Rault, J. Phys.: Condens. Matter **15**, S 1193 (2003).
44. J. Rault, J. Non-Cryst. Solids **357**, 339 (2011).
45. J. Rault, J. Non-Cryst. Solids **352**, 4946 (2006).
46. N.H. Nachtrieb, Adv. Phys. **16**, 309 (1967).
47. V.A. Bershtein, V.M. Egorov, *Differential Scanning Calorimetry of Polymers* (Ellis Horwoood, Chischester, UK, 1994).
48. E. Donth, *The Glass Transition* (Springer, Berlin, 2001).
49. C. Bauwens-Crozet, J.C. Bauwens, Polymer **23**, 1599 (1982).
50. G. Adam, A. Cross, R.N.J. Haward, J. Mat. Sci. **10**, 1582 (1975).
51. W.D. Cook, M. Mehrabi, G.H. Edward, Polymer **40**, 1209 (1990).
52. C. Bauwens-Crozet, J.C. Bauwens, G. Homes, J. Polym. Sci. **7**, A-2 (1969).
53. E. Pink, H. Bouda, B.H. Bäck, Mater. Sci. Eng. **38**, 89 (1979).
54. F. Povolo, G. Schwartz, E.B. Hermida, J. Appl. Polym. Sci. **61**, 109 (1996).
55. Y. Nanzai, Prog. Polym. Sci. **18**, 437 (1993).
56. Y. Nanzai, N. Nakayama, J. Non-Cryst. Solids **172-174**, 771 (1994).
57. Y. Nanzai, ISME Int. J. A **37**, 149 (1994).
58. Y. Nanzai, T. Yamasaki, S. Yoshioka, ISME Int. J. A **41**, 31 (1998).
59. J.M. Lefebre, B. Escaig, J. Mater. Sci. **20**, 438 (1985).
60. H.W. Zhang, G. Subhash, X.N. Jing, L.J. Kecskes, R.J. Dowding, Philos. Mag. Lett. **86**, 333 (2006).
61. R.N. Haward, *The Physics of Glassy Polymers* (Applied Science Publishers Ltd, London, 1973).

62. S. Rabinowitz, I.M. Ward, J.S.C. Parry, J. Mater. Sci. **5**, 29 (1970).
63. J.A. Sauer, D.R. Mears, K.D. Pae, J. Mater. Sci. **24**, 451 (1970).
64. K.I. Tsirule, E.L. Tyunina, in *High Pressure and Physics of Polymers*, edited by A.L. Kovarskii (CRC Press, Boca Raton, US, 1994).
65. C.P.R. Hoppel, T.A. Bogetti, W. Gillepie, J. Therm. Comput. Mater. **8**, 375 (1995).
66. W.A. Spitzig, O. Richmond, Polym. Eng. Sci. **19**, 1129 (1979).
67. J.O. Chua, A.L. Ruoff, J. Appl. Phys. **46**, 4659 (1975).
68. H.B. Yu, K. Samwer, Y. Wu, W.H. Wang, Phys. Rev. Lett. **109**, 095508 (2012)